THE MECHANISM OF FRACTURED SANDSTONE IN COMPACTION CREEP PROCESS

by

Zhanguo MA* *, Minchao ZHANG, Shixing CHENG, Jun HU, Yang SU, and Yongheng CHEN

State Key Laboratory for GeoMechanics and Deep Underground Engineering,
School of Mechanics and Civil Engineering,
China University of Mining and Technology, Xuzhou, China

Original scientific paper
https://doi.org/10.2298/TSCI180823251M

In this paper, we construct the true contour of the broken rock for the first time. Moreover, we reproduce the 2-D accumulation pattern and realize the numerical simulation transformation of the compressive creep test of the broken rock. It is shown that the simulation results are in good agreement with the laboratory tests. The research shows that the smaller the particle size, or the higher the stress, the easier it is for creep breakage to occur.

Key words*: particle flow, broken rock, creep, force chain*

Introduction

In engineering sector and nature, the crushed rocks widely exist many gaps in the natural accumulation state. The load causes a deformation of the crushed rocks, and decreases the volume of the voids, which is accompanied by creep over time. The creep behavior of crushed rocks can cause surface subsidence in a worked-out section, rail deformation, and instability in a foundation, slope, or dam [1]. The change in the void ratio of crushed rocks, which was caused by creep, affect the seepage of the groundwater, leads to a groundwater inflow and other disasters in mining and tunnel excavation projects. For the intact and crushed rocks, the creep Mechanism, creep model, and test methods have been studied in depth, although studies on the creep occurring in crushed rocks remain in the exploratory stage.

Crushed rocks have been widely used as the filling material in a worked-out section, which cannot only avoid the destruction of land through coal mining but also reduce environmental pollution. The rocks are compressed and fractured in the worked-out section, and their mechanical properties therefore change. Thus, studies on the compression and deformation of crushed rocks are important regarding the process of green coal mining.

Based on a compaction experiment on crushed rocks [2], it was found that their compactness is clearly different from that of ordinary soil. Crushed rocks generally undergo particle breakage and changes in gradation. Compared with crushed rocks before rolling, the macroscopic mechanical properties will clearly change. If the mechanical parameters before rolling are used in the calculation, the results will differ significantly from the actual stress and deformation. The relationship among the gradation, crack propagation, and peak strength from a microscopic perspective has been studied [3]. The simulation of a rolling crushed rock

* Corresponding author, e-mail: 1044@cumt.edu.cn

mass and its shape have also been discussed [4]. The filling body is permanently buried in the worked-out section, and the creep effect becomes increasingly clear over time. This leads to surface subsidence and other hazards. For this purpose, the influence of rock mass creep on the surface subsidence has been reported [5]. The creep effect of gravel filling of different sizes based on a field experiment, the fitting equation of the displacement curve, and the excursion effect in the curve have been proposed [6]. In addition, the creep characteristics of the coarse-grained soil in a landslide body were considered through a laboratory experiment [7]. Because it is difficult to detect the stress distribution characteristics of the internal rock particles and the crack growth, it is impossible to explore the mechanism of an internal excursion. In contrast, with the use of a numerical test method, we can directly study the compaction effect of crushed rocks. The discrete element method (DEM) has also been widely used to study the creep behavior of discontinuous rocks. Studies on the failure mode and material process have shown clear advantages compared with other numerical methods.

In the present paper, taking fractured sandstone as an example, the DEM based on the particle flow code (PFC) [8] is applied to establish the numerical and fragmentable cluster models, and to study the creep effect of crushed rocks during compaction at the mesoscopic level.

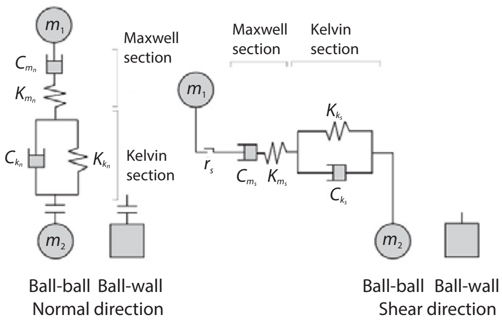

Figure 1. The Burgers contact model

Particle flow model of fractured sandstone

Introduction of Burger's model

In PFC [8], the contact between particles will produce a force, as shown in fig. 1. Such contact can be divided into normal and tangential contact forces. These two directions are made up of Kelvin and Maxwell models used in-series. Under normal contact, the Kelvin model includes a linear spring, denoted as K_{kn} and viscous element, denoted as C_{kn}. The Maxwell model includes a parametric linear spring, denoted as K_{kn} and viscous element, denoted as C_{kn}. Under tangential contact, the Maxwell model includes C_{ms} and K_{ms}, and the Kelvin model includes K_{ks} and C_{ks}. A slider with friction coefficient r_s limits the value of the shear force according to the Coulomb law.

The displacement relationship between the ball-ball or ball-facet in the model is given:

$$u = u_k + u_{m_k} + u_{m_c} \tag{1}$$

where u is the total displacement, u_k – the total displacement of the Kelvin model, u_{m_k} – the elastic element displacement in the Maxwell model, and u_{m_c} – the cohesive element displacement in the Maxwell model.

By seeking the derivative of eq. (1) with respect to the time:

$$\begin{aligned} \dot{u} &= \dot{u}_k + \dot{u}_{m_k} + \dot{u}_{m_c} \\ \ddot{u} &= \ddot{u}_k + \ddot{u}_{m_k} + \ddot{u}_{m_c} \end{aligned} \tag{2}$$

For the Kelvin model, the force and displacement can be written:

$$f = \pm K_k u_k \pm C_k \dot{u}_k$$

and

$$\dot{f} = \pm K_k \dot{u}_k \pm C_k \ddot{u}_k \tag{3}$$

where f is the force at both ends of the model, K_k – the stiffness of the elastic element, C_k – the stiffness of the viscous element, and u_k represents the displacement in the Kelvin model.

For the Maxwell model, we have:

$$\begin{aligned} f &= \pm K_m u_{m_k} \\ \dot{f} &= \pm K_m \dot{u}_{m_k} \\ \ddot{f} &= \pm K_m \ddot{u}_{m_k} \\ f &= \pm C_m \dot{u}_{m_c} \\ \dot{f} &= \pm C_m \ddot{u}_{m_c} \end{aligned} \tag{4}$$

where K_m and C_m are the stiffness of the elastic and viscous elements, and u_{m_k} and u_{m_c} – the displacements of these elements, respectively.

From eqs. (2)-(4) the two-order differential equation of the Burger's model can be given:

$$f + \left[\frac{C_k}{K_k} + C_m\left(\frac{1}{K_k} + \frac{1}{K_m}\right)\right]\dot{f} + \frac{C_k C_m}{K_k K_m}\ddot{f} = \pm C_m \dot{u} \pm \frac{C_k C_m}{K_k}\ddot{u} \tag{5}$$

Mathematical model

The size of the model is 100 mm (L) × 128 mm (W). As shown in fig. 2, the walls on both sides and the bottom of the model were constructed as fixed boundaries. The loads applied to the top of the model are 4 MPa, 8 MPa, and 12 MPa, respectively. To achieve the loading stress, the displacement loading was used during the early stage. After the target stress was reached, the servo control program was written using Fish language, and the force was unchanged during the loading for the creep.

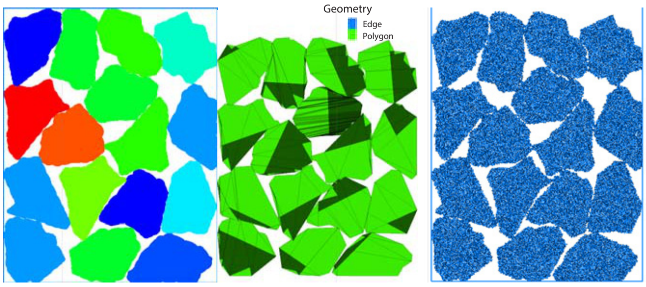

Figure 2. The stacking model in PFC

During the simulation, the shape of the crushed rocks was taken from the real shape of gangues. Considering the calculation speed, to obtain the stacking form more quickly, a clump with the same contour as the rocks was first obtained, and the entire contour of the crushed rocks was obtained using a gravity descent method. After the geometry format was exported and stored in the PFC using the *clump export geometry* command, the clump was removed and the geometry was filled with spherical particles to obtain the cluster. Burger's model was used as the ball contact in the rocks, and the contact model between rocks was linearly non-cohesive. However, the PFC cannot directly identify the rock contour. That is, we were unable to set the linear model at the joints of the rocks, and thus applied the Burger's model at the other positions. To assign the corresponding model to each contact, all contacts were first designated as the Burger's model, as shown in fig. 3(a). The DFN grid was then imported. The grid

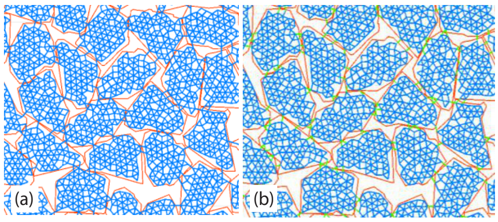

Figure 3. The contact models among rock particles; (a) before changing contact model (b) after changing contact model

shape is the geometry derived as the contour of the rock. The DFN was set as a linear model. That is, the contact passing through the DFN grid was changed into a linear model. The DFN grid was removed. A *cmat default* order was used to make a newly generated contact during the operation of the linear model, and the setting of the contact model was completed, as shown in Figure 3(b). The contact represented by the short blue line in the image is the Burger's model, the contact represented by the green line is the linear model, and the contact represented by the red line is the DFN grid.

To study the effects of the particle size on the rock disintegration and breakage, five different sizes were adopted, as shown in tab. 1.

Table 1. The particle size of the crushed rock

Grade	S_1	S_2	S_3	S_4	S_5
Particle size	20-25	15-20	10-15	5-10	2.5-5

Before the Burger's model was applied in the numerical experiment, we needed to adjust the parameters. Correct and reasonable parameters were obtained through inversion using the control variable method. The complete gangue samples with a diameter of 50 mm and a height of 100 mm were selected for the creep test. In this study, an experiment was conducted using crushed rocks and the parameters of the numerical simulation assigned to each rock. Therefore, only a complete rock creep test was required as a control. Through repeated calibrations of the laboratory creep experiments, the microscopic parameters of the rocks in tab. 2 were obtained. A comparison between the experimental curve and the simulation results of a gradation loading is shown in fig. 4.

Table 2. Microscopic parameters of the sandstone materials

Parameters	Value	Parameters	Value
Minimum particle radius [mm]	0.3	C_{ks}	4.2e9
Particle size ratio	0.15	K_{mn}	1.2e15
Particle density	2350	C_{ms}	4.3e8
C_{kn}	4.5e8	K_{ms}	1.2e15
K_{ks}	1.4e7	K_{kn}	1.6e15
K_{ms}	1.0e6	Friction coefficient	0.35

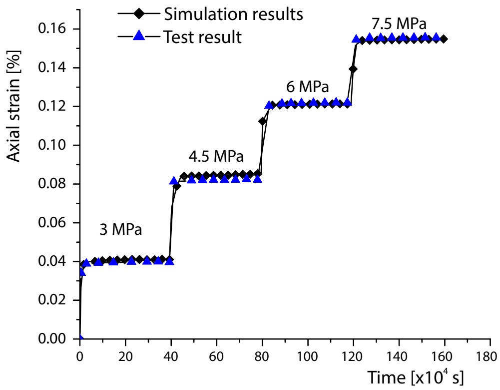

Figure 4. Comparison of the strains between step loading simulation and experiment

Analysis of numerical simulation results

Effect of particle diameter on displacement

As shown in fig. 5, the relationship between displacement and time under different sieving particle sizes are given. With the increase in sieving particle size, the displacement of the creep initiation point correspondingly increases, which indicates that the rearrangement and crushing compaction (primary crushing) of the particles takes place when displacement loading is used to reach the target stress state. This process is clearer with an increase in the particle size. During a creep state, the load remains unchanged. During the early stage of creep, the displacement clearly changes, increasing over time, and gradually stabilizes. However, for certain

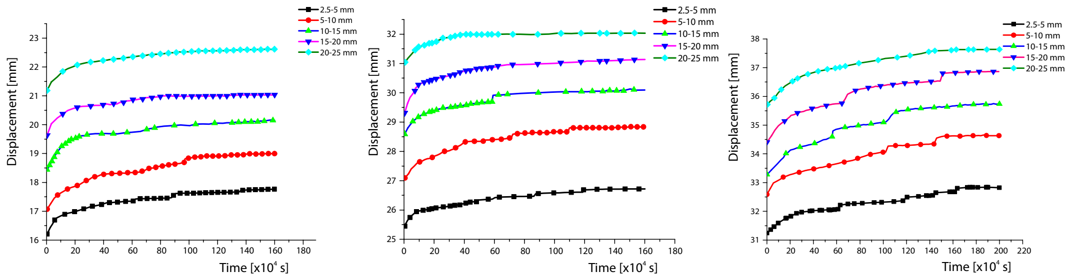

Figure 5. The relationship between displacement and time under different sieving particle sizes

sieving particle sizes, the displacement curve will have jumping points (displacement excursion), which indicates that the crushed rocks will break twice during the later stage of creep. As shown in the image, smaller particle sizes are more likely to have a displacement excursion under the same state of stress. At 4 MPa of stress, particle sizes S_4 and S_5 have a displacement excursion, whereas a particle size of S_1-S_3 does not have such an excursion. Compared with 8 MPa and 12 MPa, if a displacement excursion occurs, the range of particle sizes of secondary crushing increases with the increase in stress. At 8 MPa, the particle size of secondary crushing is S_3-S_5. At 12 MPa, the range of the particle size of secondary crushing is S_2-S_5. Among them, the displacement curves for a particle size of S_5 at 4 MPa, 8 MPa, and 12 MPa have one, two, and three excursions, respectively. The average excursion ratio (the ratio of excursion displacement to pre-excursion displacement) is 1.4%, 0.7%, and 0.5%, respectively. The displacement curves for a particle size of S_4 at 4 MPa, 8 MPa, and 12 MPa have one, two, and two excursions, respectively. The average excursion rate is 1.1%, 1.03%, and 0.9%, respectively. The displacement curves for a particle size of S_3 at 4 MPa, 8 MPa, and 12 MPa have zero, one, and two excursions, respectively. The average excursion rate is 0%, 1.3%, and 0.9%, respectively. Thus, the excursion rate decreases with an increase in stress.

Evolution law of gradation

During the loading process, whether in the stage of displacement loading or in the process of force loading creep, the breakage of rock particles directly changes the gradation of the crushed sandstone, and significantly affects the change in gap ratio. Obtaining the change law of gradation through statistics is extremely important for verifying the reliability of the model and exploring the causes of changes of displacement and the gap ratio.

Because of the complex shape of crushed rocks during the experiment, it is difficult to define the particle size of the cracked and crushed sandstone. The equivalent size of each fragment, denoted as D_m, can be represented:

$$D_m = 2\sqrt{\sum_{i=1}^{n} r_i^2} \tag{6}$$

where r_i is the size of a single spherical particle constituting fragments, and n – the number of spherical particles.

As shown in fig. 6, the gradation of particle sizes of S_1, S_3, and S_5 are at stress levels of 4 MPa, 8 MPa, and 12 MPa before and after creep, respectively. The curve shows that, under a load, the original single-grain gradation in the model evolves into a continuous gradation. The gradation curve is S-shaped on the whole. To explore the change in gradation under a load, we introduce the coefficient of inhomogeneity, denoted as C_u, *e. g.*:

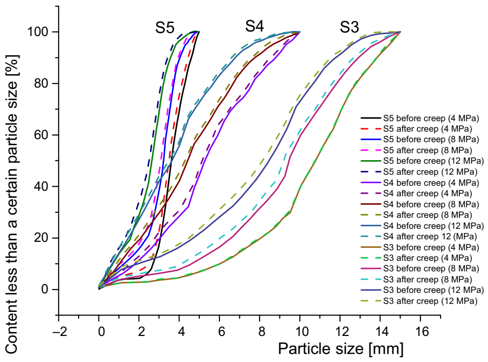

Figure 6. The gradation plot before and after creep

$$C_u = \frac{d_{60}}{d_{10}} \tag{7}$$

where d_{60} is the particle size accounting for 60% of the sieving weight, and d_{10} – the particle size accounting for 10% of the weight. The coefficient of inhomogeneity is the ratio of limited particle size to the effective particle size, which reflects the degree of homogeneity of the soil particles. The greater the degree of homogeneity, the smaller coefficient of inhomogeneity is and the simpler the particle size. As shown in tab. 3, the values of the coefficients of inhomogeneity at different sieving particle sizes and different load levels are presented.

Table 3. The values of the coefficients of inhomogeneity before and after creep

No.	4 MPa (before creep)	4 MPa (after creep)	8 MPa (before creep)	8 MPa (after creep)	12 MPa (before creep)	12 MPa (after creep)
S_1	2.14	2.14	3.45	3.45	5.13	5.13
S_2	1.93	1.93	4.02	4.02	4.98	5.09
S_3	1.84	1.93	2.14	2.47	4.54	5.56
S_4	1.69	1.74	2.48	2.69	4.63	5.28
S_5	1.41	1.52	2.62	2.80	4.57	4.71

Force chains characteristics

As shown in fig. 7, the distributions of the force chains in the rock particles in the force chain of the samples with a sieving particle size of 15-20 mm are presented. The contact point of the crushed sandstone is the stress concentration point. The stress in the area surrounded by the contact points is relatively high. For a crushed rock mass with only two contact points, the force chain is spindle-shaped, and the two ends of the spindle are the contact points of the crushed sandstone.

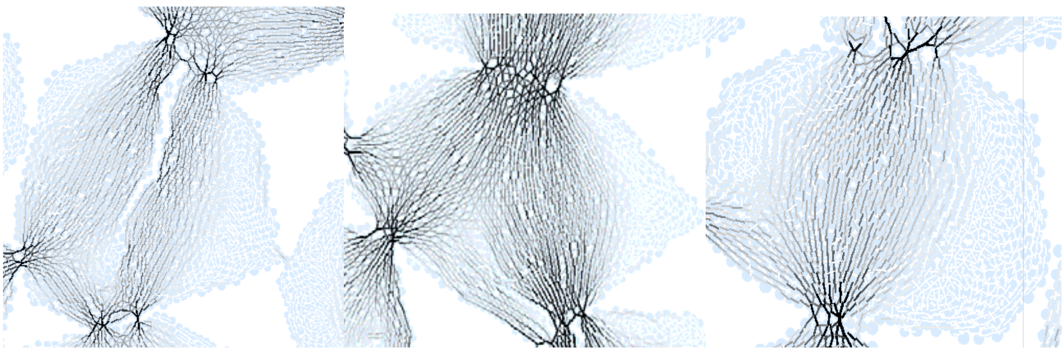

Figure 7. Distributions of the force chains in the rock particles

Conclusion

In the present task, the true contour of the broken rock have been proposed for the first time. We reproduced the 2-D accumulation pattern and realized the numerical simulation transformation of the compressive creep test of the broken rock. According to the displacement curve, the smaller the particle size, or the higher the stress, the easier it is for creep breakage to occur. The ratio of displacement excursion caused by the breakage decreases with an increase in the stress level. The excursion rate decreases with an increase in stress. With the rearrangement and breakage of particles, the grain size gradation of rocks becomes more continuous, the void ratio decreases, and the rearrangement of particles is finally inhibited. The stress in the area in contact with the contact points is relatively high. For a crushed sandstone in contact with only two contact points, the force chain is spindle-shaped. The simulation results are in good agreement with the laboratory tests. It is shown that the smaller the particle size, or the higher the stress, the easier it is for creep breakage to occur.

Acknowledgment

This work is supported by the National Natural Science Foundation of China (No. 51674250); Major Program of National Natural Science Foundation of China (No. 51734009).

Nomenclature

C_k – stiffness of the viscous element, [Nm^{-1}]
C_m – stiffness of viscous elements, [Nm^{-1}]
C_u – coefficient of inhomogeneity, [–]
D_m – equivalent particle diameter, [m]
d_{10} – particle size accounting for 10%, [m]
d_{60} – particle size accounting for 60%, [m]
f – force at both ends of the model, [N]
K_k – stiffness of the elastic element, [Nm^{-1}]
K_m – stiffness of the elastic elements, [Nm^{-1}]
r_i – radius of spherical particles, [m]
u – total displacement, [m]
u_k – displacement in the Kelvin model, [m]
u_{m_c} – cohesive element displacement, [m]
u_{m_k} – elastic element displacement, [m]

Reference

[1] Gong, P., *et al.*, Floor Heave Mechanism of Gob-Side Entry Retaining with Fully-Mechanized Backfilling Mining, *Energies*, *12* (2017), 10, 2085
[2] Gong, P., *et al.*, An Experimental Investigation on the Mechanical Properties of Gangue Concrete as a Roadside Support Body Material for Backfilling Gob-Side Entry Retaining, *Advances in Materials Science and Engineering*, *2018* (2018), ID 1326053
[3] Zhang, J., *et al.*, Geometric Anisotropy Modelling and Shear Behavior Evaluation of Graded Crushed Rocks, *Construction and Building Materials*, *183* (2018), 1, pp. 346-355
[4] Jiang, Y., *et al.*, A Numerical Test Method of California Bearing Ratio on Graded Crushed Rocks Using Particle Flow Modelling, *Journal of Traffic and Transportation Engineering (English Edition)*, *2* (2015), 2, pp. 107-115
[5] Shi, X., *et al.*, Influences of Filling Abandoned Salt Caverns with Alkali Wastes on Surface Subsidence, *Environmental Earth Sciences*, *73* (2015), 11, pp. 6939-6950
[6] Ma, Z., *et al.*, Experimental Study on Creep Behavior of Saturated Disaggregated Sandstone, *International Journal of Rock Mechanics and Mining Sciences*, *66* (2014), Feb., pp. 76-83
[7] Di Maio, C., *et al.*, Residual Strength and Creep Behaviour on the Slip Surface of Specimens of a Landslide in Marine Origin Clay Shales: Influence of Pore Fluid Composition, *Landslides*, *4* (2015), 12, pp. 657-667
[8] ***, Itasca Consulting Group Inc., PFC2D (Particle Flow Code in 2D), Version 5.0, Minneapolis: Itasca Consulting Group Inc., 2016

Paper submitted: August 23, 2018
Paper revised: November 11, 2018
Paper accepted: January 12, 2019